Construction and Building Materials 230 (2020) 117056

Contents lists available at ScienceDirect

Construction and Building Materials

journal homepage: www.elsevier.com/locate/conbuildmat

Performance of crystalline forming additive materials in concrete

Mona Elsalamawy, Ashraf R. Mohamed, Abdel-latif E. Abosen *

Structural Engineering Department, Faculty of Engineering, Alexandria University, 21544, Egypt

HIGHLIGHTS

- Different phases of calcium silicate hydrate have been formed in presence of CA materials.
- EDX analysis depicted that the formed crystals was C-S-H having high C/S ratio.
- Great reduction in the pores diameters and water capillary raise resistivity in presence of CA.
- Presence of CA is not pronounced in case of concrete with low *w/c*.
- Continuous water curing lead to enhancement of the concrete impermeability in case of using CA.

ARTICLE INFO

Article history:
Received 18 June 2019
Received in revised form 14 September 2019
Accepted 20 September 2019

Keywords:
Crystalline additive materials
Ca/Si ratio
Pores blocking
Microstructure
SEM
EDX
Sorptivity

ABSTRACT

Crystalline forming materials have shown a considerable reduction in permeability of concrete structures under severe environment. This paper addresses the performance of crystalline forming additive materials in terms of morphology characterization and water Sorptivity. Three different water-cement ratios of concrete; namely, 0.6, 0.5 and 0.387 have been considered to cover the range of concrete mixtures from highly to low permeable concrete. Test methods include scanning electron microscopy (SEM), coupled with energy-dispersive X-ray spectroscopy (EDX), thermo-gravimetric analysis (TGA), X-ray diffraction (XRD) and sorptivity test. The results indicate that, the potential of crystalline materials to reduce permeability of concrete depends on available pore space in concrete mixtures. Thus, the effectiveness of these materials appears in high water cement ratio mixtures. The crystals have been found to be calcium silicate hydrate "C–S–H" of different phases ranging from round to needle form with high Ca/Si ratio.

1. Introduction

Severe environmental conditions usually result in concrete deterioration. This deterioration is mainly attributed to connectivity of inner pores of concrete microstructure. Thus, the network and structure of these pores represent the cornerstone of concrete durability and mechanical properties which may alter the service life of concrete structures [1].

Currently, crystalline forming additive materials (CA) are widely used to reduce concrete permeability (ACI 212) [2]. It has been postulated by many researches [3–7] and even with the materials manufactures that these materials have the ability to seal the concrete surface by filling the concrete cracks and large pores with insoluble crystalline materials. Moreover, these materials also have the ability to heal cracks autogenously [8–12].

This paper addresses the chemical composition and morphology of these crystals with an emphasis on the source and condition of their formation. This has been accomplished through several experimental techniques for quantitative and qualitative characterization of the crystalline phase forming process. These techniques include microscopic evaluation such as scanning electron microscopy, (SEM) coupled with energy-dispersive X-ray spectroscopy (EDX), and macroscopic evaluation such as thermo-gravimetric analysis (TGA), X-ray diffraction (XRD), and Sorptivity testing.

2. Experimental program

2.1. Materials and concrete mixtures

CEMI 42.5N Portland cement, with properties shown in Table 1, has been used throughout this study. Aggregate includes crushed pink limestone of 19 mm nominal maximum size, natural sand

* Corresponding author.
E-mail address: abdellatif.elsayed@alexu.edu.eg (Abdel-latif E. Abosen).

https://doi.org/10.1016/j.conbuildmat.2019.117056
0950-0618/

Table 1
Chemical and Phases Composition of used CEMI 42.5 N.

Chemical Compositions	SiO_2	CaO	Fe_2O_3	Al_2O_3	MgO	K_2O	Na_2O	SO_3	CO_2
Percentage (wt. %)	19.48	62.36	3.78	4.1	2.31	0.31	0.41	2.32	1.5
Calculated Phase Composition (ASTM C 150)									
Cement Phase Composition	C_3S	C_2S	C_3A	C_4AF					
Percentage (wt. %)	58	12	4.4	12					

Table 2
Mixture proportion.

Mixes	Water/cement ratio (*w/c*)	Cement Content (Kg/m^3)	Aggregates (Kg/m^3)	CA1	CA2	CA3	Super plasticizer (% of cement wt.)
Mix 1	0.60	350	1694	–	–	–	0.50%
Mix 2	0.50	350	1780	–	–	–	1.00%
Mix 3	0.387	350	1884	–	–	–	1.50%
Mix 4	0.60	350	1694	2%	–	–	0.50%
Mix 5	0.50	350	1780	2%	–	–	1.00%
Mix 6	0.387	350	1884	2%	–	–	1.50%
Mix 7	0.60	350	1694	v	2%	–	0.50%
Mix 8	0.50	350	1780	–	2%	–	1.00%
Mix 9	0.387	350	1884	–	2%	–	1.50%
Mix 10	0.60	350	1694	–	–	2%	0.50%
Mix 11	0.50	350	1780	–	–	2%	1.00%
Mix 12	0.387	350	1884	–	–	2%	1.50%

(with fineness modulus of 2.63), and high range water reducing admixture (HRWR).

Three different sources of the commercially produced crystalline additives materials (CA) were used, at a dosage equal to 2% by cement weight (according to the manufacturers' recommendations), named CA1, CA2 and CA3.

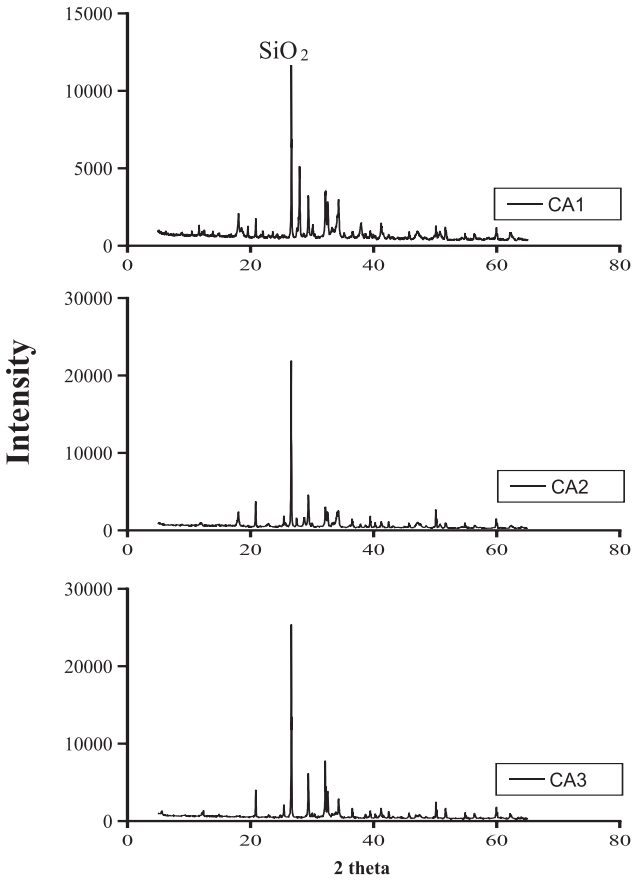

Fig. 1. XRD Pattern for Different Crystalline Additives Materials.

With respect to concrete mixtures, Table 2 shows the composition of mixes used in this study. The significant variation of w/c reflects the wide range of concrete mixtures from highly to low permeable concrete.

2.2. Mineralogical analysis for CA materials

XRD was conducted for the powder specimens of CA materials, the results showed that, the strongest peak position for the crystalline materials is centred on (2θ) equal to 26.6° with different intensities as illustrated in Fig. 1. This peak is corresponding to the (2θ) reflection of silicon dioxide (SiO_2). The mineralogical composition of the three investigated CA materials obtained by means of XRD analysis is summarized in Table 3. The results revealed that, the crystalline additives materials (CA) are mainly composed of cement, silica and carbonated materials as reported in XRD analysis. These materials have similar mineral gradients with different percentage as shown in Fig. 1. Moreover, it may be noted also that, CA1 crystalline materials containing lower content of SiO_2 compared to CA2 and CA3 as indicated in XRD analysis.

2.3. Qualitative and quantitative procedure

Two different approaches have been considered in this research; qualitative (SEM) and quantitative (EDX, TGA/DTG and XRD). SEM has been used to identify the morphology of the formed crystals, if any, and their different structure. EDX uses the SEM images to identify the different phases of the formed crystals based on elemental analysis. Furthermore, TGA/DTG analysis has been utilized to check the reactivity of the CA materials with the cement

Table 3
Mineralogical analysis for crystalline additives materials.

Candidate	Formula	CA1	CA2	CA3	Used Cement
Silicon oxide [Quartz]	SiO_2	32.840	44.971	48.36	19.48
Portlandite	$Ca(OH)_2$	7.505	6.684	7.825	–
Alite (C_3S)	–	28.527	26.468	20.623	58
Larnite (C_2S)	–	31.128	21.877	23.192	12

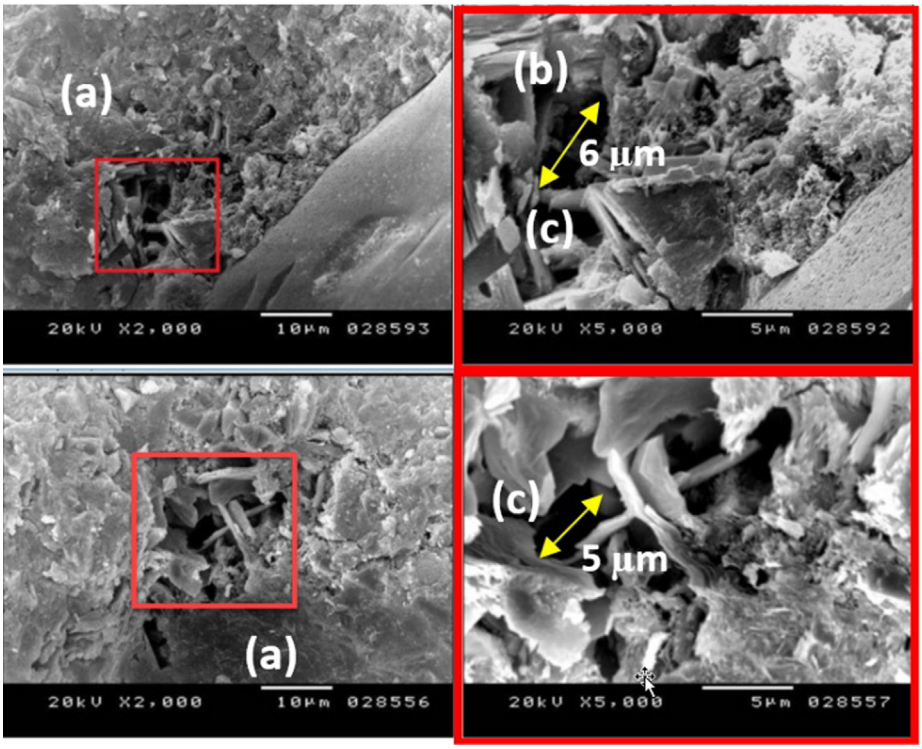

Fig. 2. SEM images for cement mortar without crystalline additives materials (a) typical C–S–H phase, (b) typical portlandite Phase and (c) cavities (~5 µm).

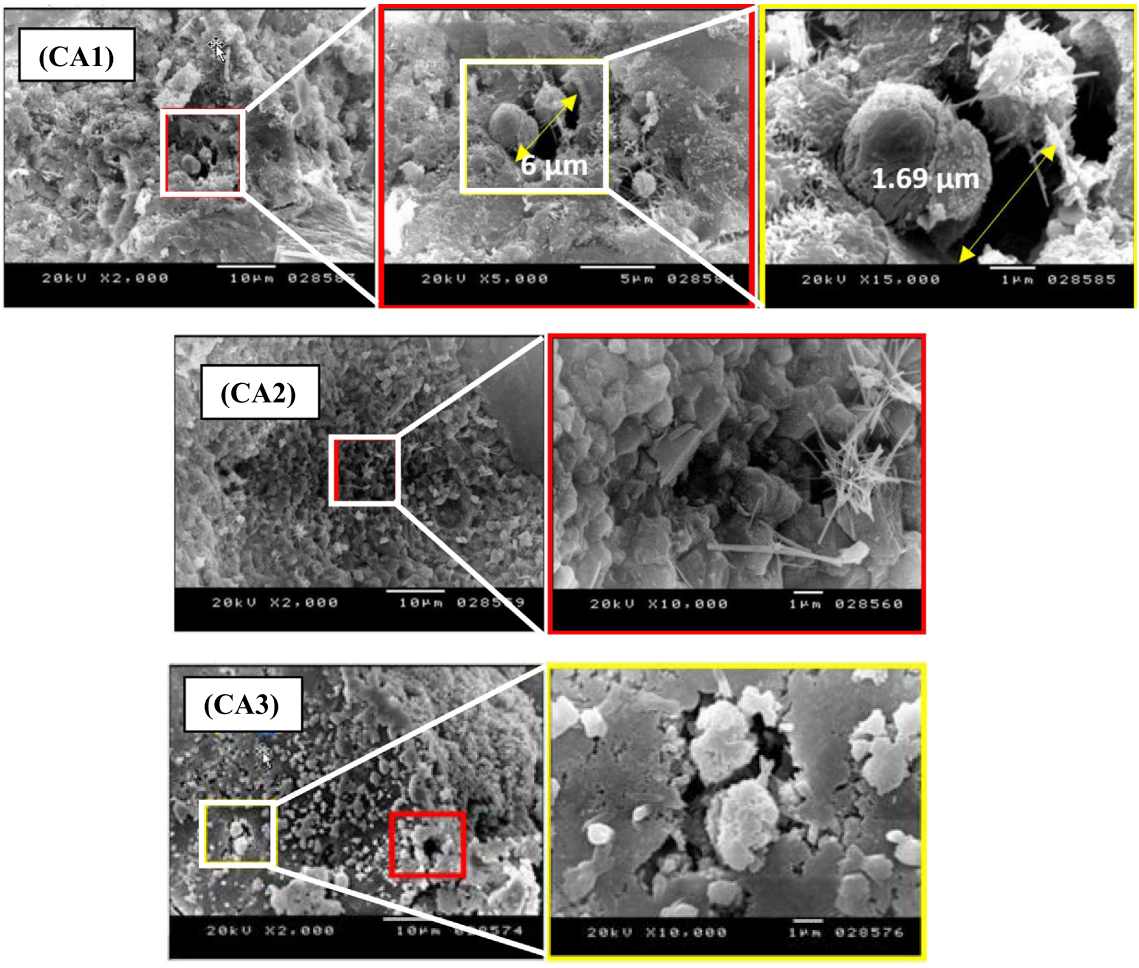

Fig. 3. SEM images for cement mortar with different crystalline additives materials (CA1, CA2 and CA3).

hydration product. On the other hand, performance characterization of these materials has been evaluated through Sorptivity testing (ASTM C1585-13) [13]. All samples were subjected to water curing condition until being tested.

2.4. Specimen preparation

2.4.1. Morphology characterization specimens

All specimens were prepared out of the concrete mortar through sieving the fresh concrete mix using No.4 ASTM C 33 sieve. The sieved mortar was cast in prisms ($50 \times 50 \times 200$ mm) for testing.

The morphology analysis investigation using SEM and EDX of the newly broken surface, were taken from the pre-prepared prisms at 14 and 28 days, for all specimens.

For thermo-gravimetric analysis (TGA/DTG), powder samples of 20 mg were prepared at tested ages, at 7, 14 and 28 days, from newly broken samples by grinding and sieving it using mesh opening of (75 μm).

In addition, (TGA/DTG) analysis was conducted on hydrated paste of CA materials mixed with either water or simulated concrete pore solution. That is to disclose the reactivity of CA materials with the cement alkali that exists in pores. Where, simulated pore solution of cement is the output of the filtering the paste prepared by adding deionized water to cement powder by 0.45 ratio by weight after 1.5 min of mixing [14]. For this elucidation, (TGA/DTG) was conducted on these pastes after 7 days only.

2.4.2. Performance characterization specimens

Capillary rise water absorption (Sorptivity) cylindrical specimens (100×200 mm) were cast. then after 7 days of water curing, these specimens were cut into individual specimens of (50 mm) height from the center of the original specimen according to ASTM C1585-13 [13]. In this test method, only one surface is exposed to water at room temperature while the other surfaces are sealed

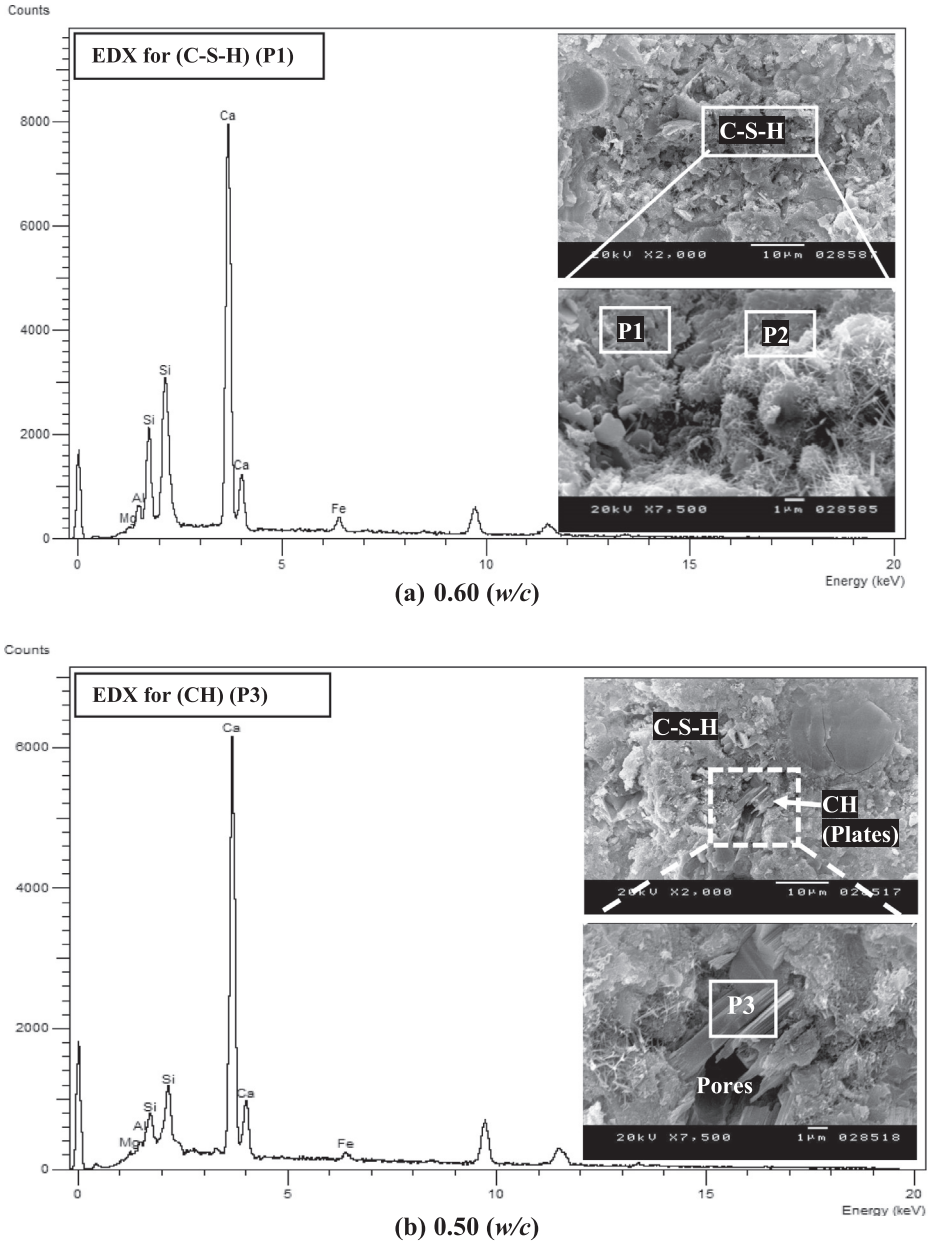

Fig. 4. SEM/EDX Images for Control Samples at different Magnification; top (X2000) and bottom (X7500).

simulating water absorption in a member that is in contact with water on one side only. After cutting the test specimens "100 mm in diameter and 50 ± 3 mm in length" all the specimens were saturated using vacuum saturation procedure, then the specimens were placed for 3 days in desiccator inside an oven at 50 ± 2 °C temperature, after that, each specimen was placed separately in a sealable container for 15 days then the specimen side sealing was installed before the start of the absorption procedure.

2.4.3. Curing conditions

All concrete specimens were initially water cured for 7 days after being demolded at room temperature, then the specimens were exposed to water curing till time of testing periods of 14, 28 and 365 days.

3. Experimental results and discussion

3.1. Morphology of the formed crystals

Morphology of hydration products and crystals formed were analysed by means of scanning electron microscopic (SEM). The typical hydration product and available space of cement mortar without crystalline additives materials are shown in Fig. 2. It can be depicted that the morphology of hydrated calcium silicates (C–S–H) and portlandite (CH). Also, the morphology monitors the contribution of portlandite to form pores.

On the other hand, different phases of crystals, for cement mortar with crystalline additives materials (CA) have appeared in the examination of SEM images as shown in Fig. 3.

3.2. SEM/EDX and Ca/Si ratio

3.2.1. Typical hydration products

SEM/EDX analyses were performed for all control mortar mixtures to visualize the main phases of hydration products; crystalline calcium hydroxide (CH) and amorphous C–S–H [15]. After 28 days, the morphology (SEM, EDX) of control specimens were shown in Fig. 4(a and b). The elemental analysis results using EDX for the investigated phases are presented in Table 4. The results illustrate that, there were amorphous C–S–H according to EDX results in points (P1, P2) which has a Ca/Si ratio of 1.8 [16], and hexagonal plates of Portlandite (CH) were indicated in point (P3), where the calcium (Ca) content is around 90% at this phase. While, the content of AL, Fe, and Mg element were relatively low. Moreover, porous structure with wider pores available was also found.

Table 4
EDX results for control specimens.

E–lements	point (P1) C–S–H phase	point (P2) C–S–H phase	point (P3) Portlandite (CH) phase
Ca	60.6	61.5	92.7
Si	34.6	34	4.2
AL	2.3	2.8	0.5
Fe	2.1	1.2	1.9
Mg	0.3	1.1	0.8
Sum	99.9	100	100
Ca/Si Ratio	1.75	1.8	–

3.2.2. Formed crystals for CA materials mixtures

SEM, EDX analyses were carried out for all mortar specimens containing crystalline additives materials (CA) to visualize the morphology of formed crystal structure. Moreover, after 7, 14 and 28 days, samples were monitored to trace the different phases of the formed crystal at different ages.

Two types of crystals are observed as shown in Fig. 5 irrespective of either the age of monitoring or the (*w*/*c*) ratios. In this study, they are referred to as either rounded crystals (type I) or needle like crystals (type II). These crystals are observed for all specimens with different crystalline additive materials and elemental analysis using EDX was produced to characterize theses phases.

Morphology of specimens containing CA1 after 28 days was shown in Fig. 6, where round crystals (type I) were observed. Their morphologies at higher magnification were similar to agglomerated very small particles in tens of nanometre. This was confirmed with previous studies, where 30 nm ball–like structure of C–S–H under Atomic Force Microscope (AFM) was documented [17]. The EDX analyses for (point P4, P5) that are shown in Table 5 illustrated that, the main elements, in these crystals, were calcium (Ca), silica (Si) and their average molar ratio (Ca/Si) was about 3.

Needle-like crystals product was investigated for the same specimens at the same age as shown in Fig. 7. EDX analysis was conducted on point (P6). This analysis confirmed that, the calcium and silica are the main elements with high average molar ratio (Ca/Si) of about 3.6 which is the same as rounded crystals. These elemental analysis (EDX) results are presented in Table 5. No difference was detected between the compositions of crystals type I and type II, although they have different structure and morphology. These different morphologies of C–S–H were documented in recent research, which indicated that one type of C–S–H morphology was small and dense round while the other was coarse and loose [18] and sometimes fibril like C–S–H [19].

Fig. 8 illustrate that, C–S–H whish was monitored from the same specimens containing (CA1) has (Ca/Si) ratio around 1.6 coincide with the typical ratio confirmed by Kurdowski et al. [15]. Moreover, its morphology was closed to be needle-like structure. This result confirms that, the investigated crystals were C–S–H

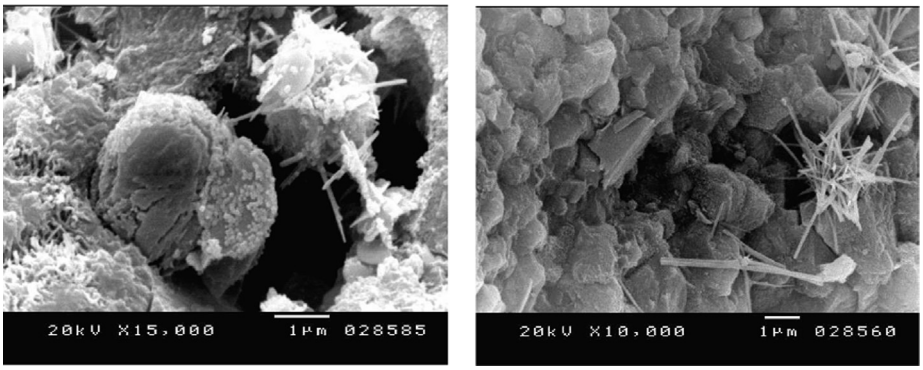

Fig. 5. SEM Images for the different types of the formed crystals left: (type I) rounded crystals, right: (type II) needle like crystals.

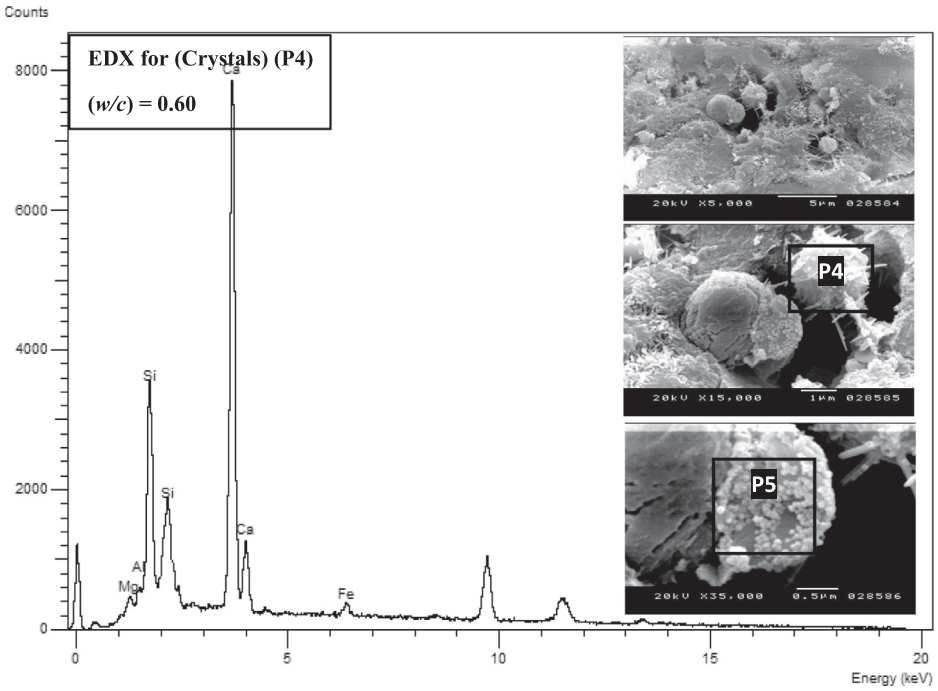

Fig. 6. SEM Images, EDX for the Crystals (rounded Crystals) magnification increasing from top to bottom.

Table 5
EDX chemical composition results for (CA1).

Elements	Points			
	(P4)	(P5)	(P6)	(P7)
Ca	73	75	72.6	58.1
Si	23.9	22.6	20	34.8
AL	0.2	0.4	2.3	0.90
Fe	1.6	1.5	4.4	4.2
Mg	1.3	0.4	0.6	1.9
Sum	100	99.9	100	99.9
Ca/Si	3.05	3.32	3.63	1.67

with different morphology due to the different of calcium and silica molar ratio. This higher ratio of Ca/Si was reported in previous studies [20]. However, the large Ca/Si variation may be due to the change of C–S–H morphology or inadequacy of the intermixing measurement of the compounds. It can thus be concluded that, with increasing Ca/Si ratios, the calcium silicate hydrate gel changes from a loose fibril-like morphology to dense granular-like particles [21].

The morphology of specimens containing CA2, and CA3 were presented in Figs. 9 and 10 for specimens with different (*w/c*) ratios. The SEM images of all concrete samples reveal the formation

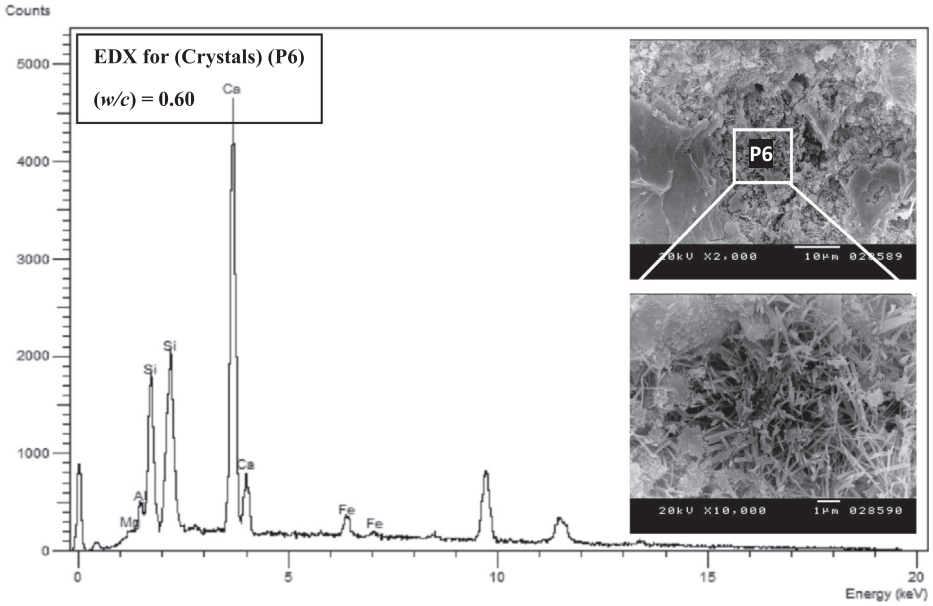

Fig. 7. SEM Images, EDX for the Crystals (Needle-like Crystals) magnification increasing from top to bottom.

of very dense structure and tiny particles. These particles are composed mainly of calcium and silica according to EDX analyses results as tabulated in Table 6 at points P8 and P9 for specimens containing CA2 and CA3 respectively. Moreover, the tiny particles had same chemical composition with round particle clusters in specimens containing CA1. In addition, the Ca/Si ratio of amorphous product, Crystals, was measured as 2.6 and 3.3 respectively.

The morphology of concrete containing (CA3) was presented in Fig. 10 for specimens with (*w/c*) of 0.6 after 14 days. The morphology presents the same crystals with Ca/Si ratio of 3.3. EDX analysis for point 9 shows that, it contains mainly (Si). So, these particles of silica may be accumulated where it plays as a nucleation zone of hydration products formation.

3.2.3. Crystals and available space

The morphology of the specimens containing CA materials investigated that, the formed crystals, whatever the age of monitoring, contributed to reduce the available space width by about 65 ± 5% as illustrated in pervious Fig. 3 and (9-a), which confirmed the high performance of concrete containing CA materials in practices. Where, the formed crystals, other phase of C–S–H gel,

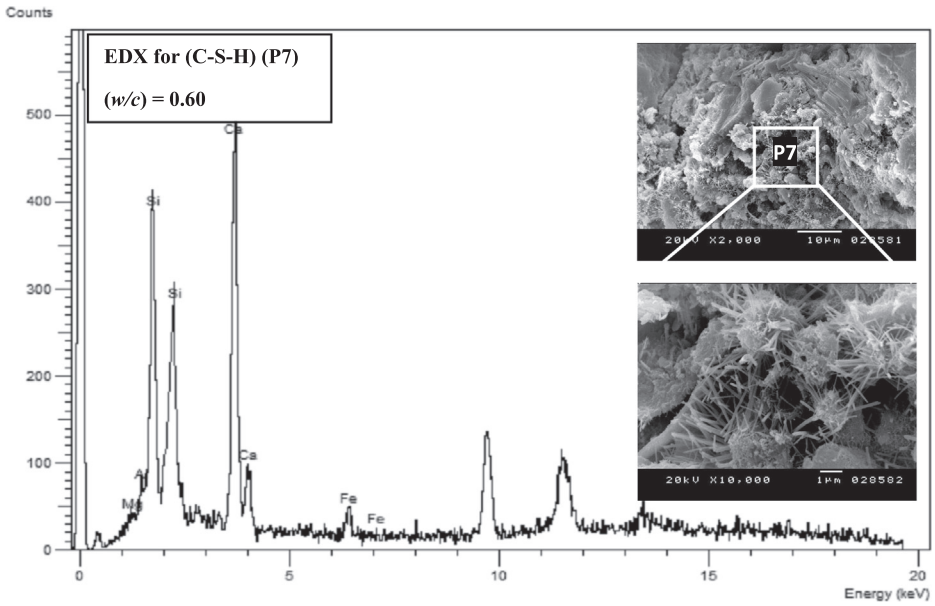

Fig. 8. SEM Images, EDX for the C–S–H magnification increasing from top to bottom.

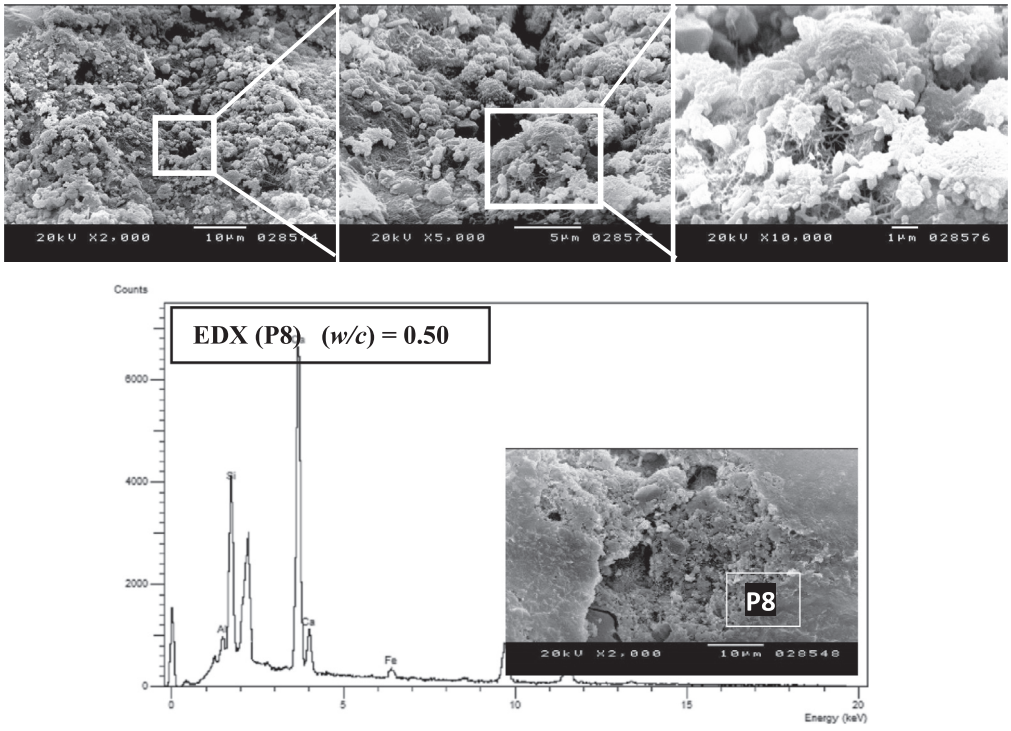

Fig. 9. (a): SEM Images, for Tiny Particles (Crystals) for specimens Contain (CA2) with 0.60 (*w/c*) after 14 Days. 9(b): SEM Images, and EDX for Tiny Particles (Crystals) for specimens Contain (CA2) with 0.50 (*w/c*) after 14 Days.

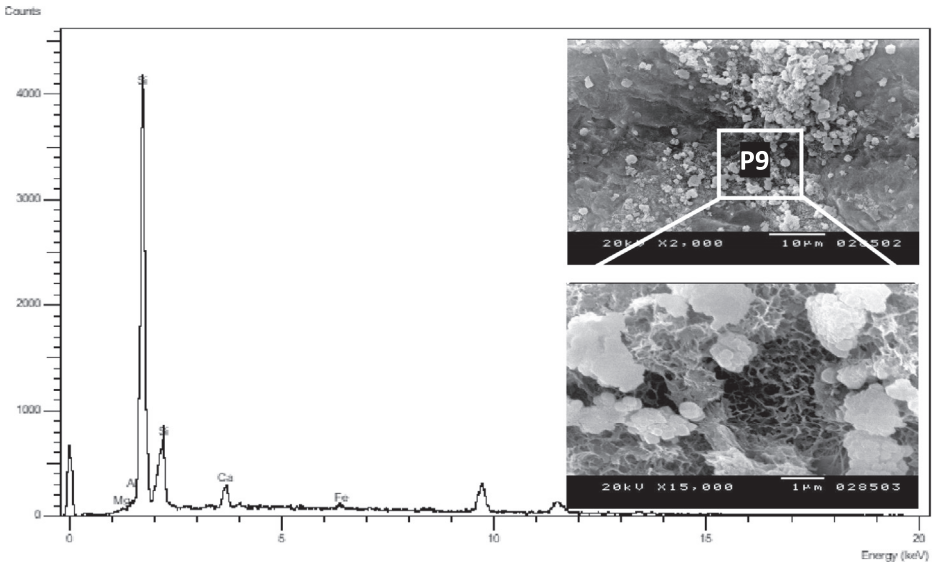

Fig. 10. SEM Images, and EDX for Crystals for specimens contain CA3 after 14 Days.

decreased the water transport of hardened concrete by partially blocking the pore structure [22].

3.3. Quantitative characterization of calcium hydroxide using TGA

Results of TG/DTG curves for CA1 hydrated either by water or simulated pore solution were shown in Fig. 11. This study indicate that endotherm peak corresponding to di-hydroxylation of (CH) usually occurs in range 375–521 °C. While, the endotherm corresponding to de-carbonation of calcium carbonate occurs over 700 °C. The results illustrated that, the portlandite (CH) content was 3.23% for specimens made of CA1 hydrated with simulated pore solution. While, this ratio reaches 7.64% when mixing CA1 with water. It may be noted that, decreasing CH content for CA mixed with pore solution leads to the reaction between silica, presented on (CA), and cement alkalis.

Table 6
EDX Chemical Composition Results for (CA2) and (CA3).

Elements	Points	
	CA2 (P8)	CA3 (P9)
Ca	65.9	74.6
Si	29.1	23
AL	2.7	0.3
Fe	2.2	1.5
Mg	–	0.2
Sum	99.9	99.8
Ca/Si	2.26	3.2

3.3.1. Effect of crystalline additive materials on CH content

The calculated CH content from TGA/DTG analysis for mortar specimens having of 0.60 and 0.50 (*w/c*) ratios with and without CA is depicted in Figs. 12, 13 respectively. These results indicate that, using CA lead to slight reduction in calcium hydroxide "CH" content. At early ages (1 days), the Nano particle acts as a nucleation site for the formation of hydration product CH and C–S–H simultaneously [23,24]. At later ages (28 days), control specimens contain higher content of CH compared to other specimens con-

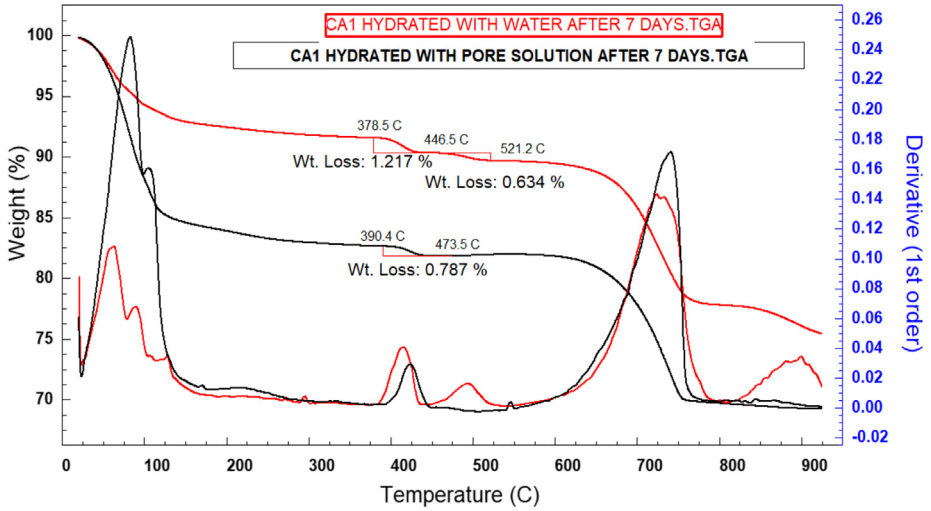

Fig. 11. TG/DTG Curve of Hydrated CA1 after 7 days.

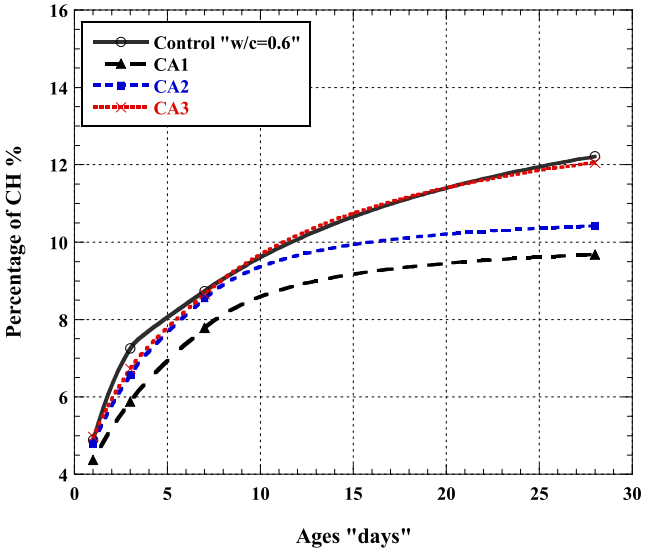

Fig. 12. Percentage of CH content with ages for specimens of 0.6 (*w/c*).

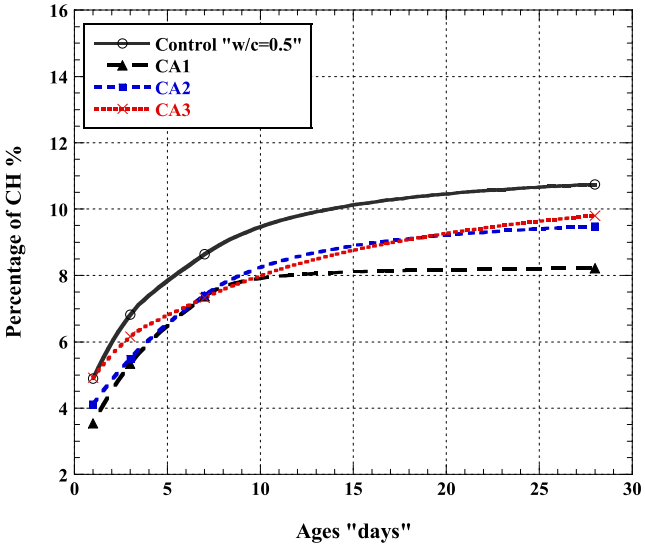

Fig. 13. Percentage of CH content with ages for specimens of 0.5 (*w/c*).

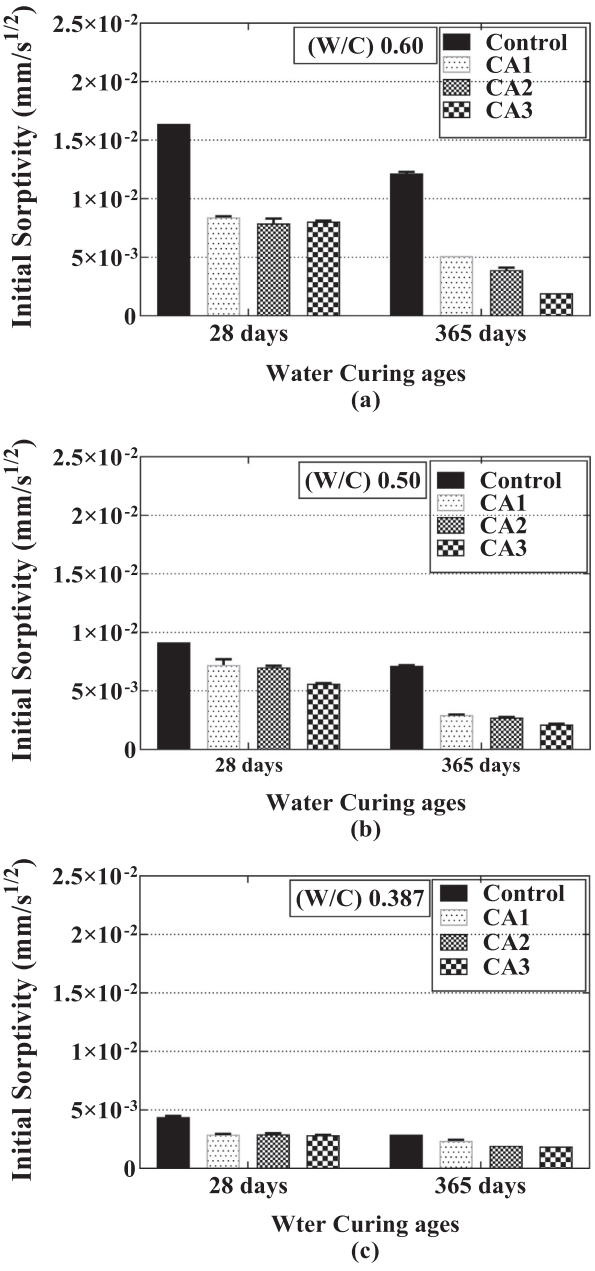

Fig. 15. Initial Sorptivity parameters for concrete specimens with and without CA with different curing ages and different (*w/c*) ratios.

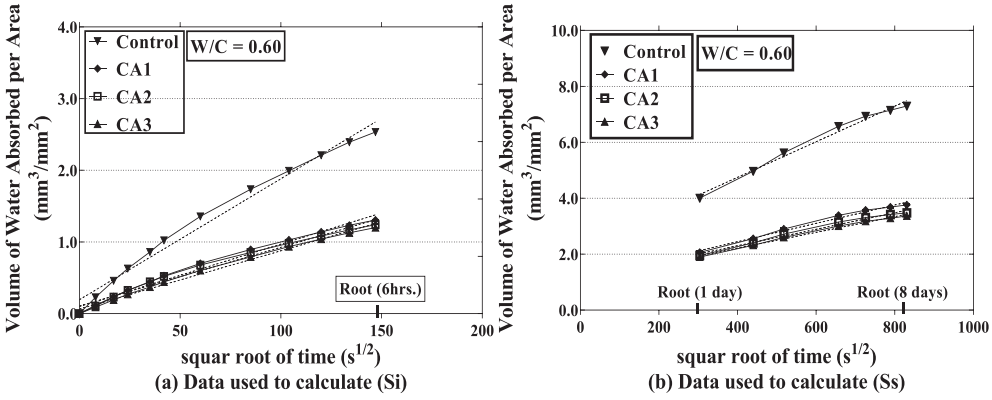

Fig. 14. (a, b) – Volume of water absorbed per cross sec area (mm^3/mm^2) vs. square root of elapsed time ($s^{1/2}$) for different (CA) materials after 28 days water curing.

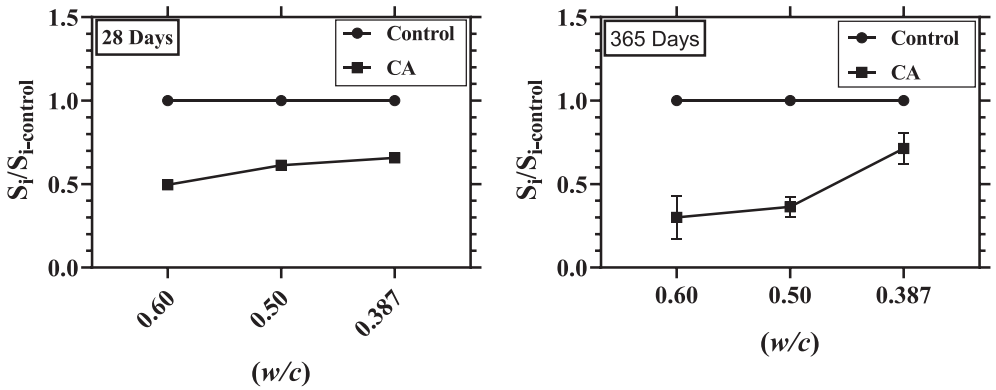

Fig. 16. Relative reduction percent in (Si) due to using CA materials in concrete after 28 and 365 water curing ages.

taining crystalline additive materials. Although all crystalline additive materials have the same composition with different ratios, CH content was varied according to type of CA materials. it was observed from figures that, concrete specimens containing CA1 has the least calcium hydroxide content compared to other types of crystalline additives materials for all concrete mixtures mentioned above. Thus, the performance of CA materials not only depends on the silica content but also its reactivity as indicated in the XRD analysis.

3.4. Capillary rise water absorption (Sorptivity)

In regard to mass change, sorptivity parameters were determined according to ASTM C1585-13 [13]. The specimen mass change was routinely measured due to water absorption at (1, 5, 10, 20, 30, 60 min and every hour up to 6 h) to determine the initial rate of water absorption (S_i), and every day until 8 days to determine the secondary rate of water absorption (S_s). These two parameters were determined by calculating the gradient of the straight-line relation between the volume of absorbed water per cross section area (I) and square root of elapsed time ($t^{1/2}$).

The sample of the measured results were provided in Fig. 14 (a, b). This figure illustrated that, there were significance reduction in volume of water absorbed per cross section are for all specimens containing crystalline additives materials (CA) compared to control specimens. In addition, the data used to calculate the secondary Sorptivity parameter (S_s) showed a systematic curvature for the control specimens.

Fig. 15 showed the calculated initial sorptivity parameters (S_i) for concrete mixtures with and without CA materials. It should be mentioned that, These parameters were not reported if the correlation coefficient less than 0.98 and the data show a systematic curvature [13]. The results showed that, there is a significant reduction in (S_i) for control specimens due to the considered curing age. This can be return to the hydration advance.

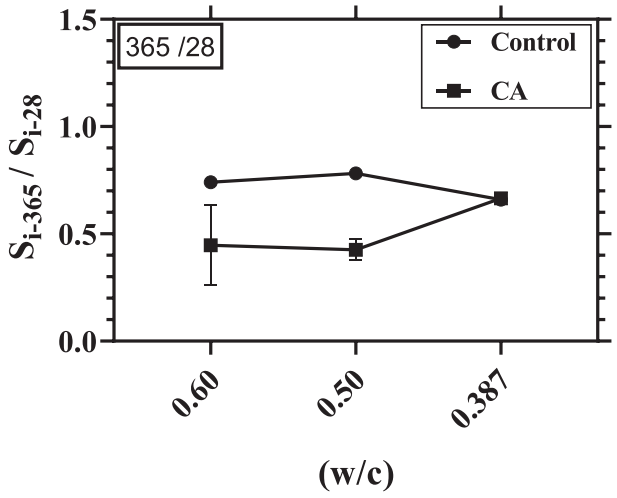

Fig. 17. Reduction percent in (Si) after 365 days water curing relative to 28 days water curing ages.

3.4.1. Dual action of hydration and crystallization

Fig. 16 showed the enhancement in resistivity of water transport with regard to (S_i) due to using CA materials relative to the control mixtures after 28, and 365 days. The results showed that, the significant effect of the using CA materials appeared with the concrete mixtures considered as a low permeable concrete, 0.60 and 0.50 (*w/c*) ratios. Where, the reduction percent after 365 days of water curing reached to about 70, 63.3, and 34.2% for concrete mixtures with 0.60, 0.50, and 0.387 (*w/c*) ratios, respectively. Moreover, these reductions were 50, 30, and 28.6% after 28 days.

The effect of prolonged water curing on Sorptivity parameters (S_i) for all concrete samples is shown in Fig. 17. The relative ratio of (S_i) after 365 days and (S_i) after 28 days for control mixtures and mixtures containing (CA) materials reveal that; highly reduction in (S_i) was observed for high permeable concrete samples, 0.60 and 0.50 (w/c) ratios, containing (CA) materials, where the reduction in (S_i) reached to approximately 60%. On the other hand, no significant enhancement in (S_i) was documented for low permeable concrete (0.387 (w/c) ratio). Thus, the use of CA is useless for concrete with low w/c.

Moreover, it is confirmed that these materials have a vital role for high permeable concrete. Whereas, the formed crystals resulted need an available space in concrete structure so by continuing water curing, the enhancement in (S_i) due to dual effect of hydration progress and formation of crystals due to presence of CA depending on available pore space. This macroscopic behaviour coincides with the morphology and microstructure characterization for concrete containing CA materials given in Section 3.2.

The above observations were confirmed with other researcher [25] which concluded that, capillary porosity was reduced significantly at early ages for silica based materials while at the later ages this reduction was not significantly.

4. Conclusion

The performance characterization of concrete containing crystalline additive materials (CA) was investigated using SEM/EDX,

TGA/DTG and sorptivity analysis. Based on the analysis it can be concluded that.

1. Different phases of calcium silicate hydrate C–S–H have been formed in presence of CA materials. These phases range from round particle to needle like crystals with Ca/Si ratio ranged from 2.4 to 3.2.
2. Crystalline additive materials have a great physical effect to reduce the size of pores, available space, where the crystals contributed to reducing pores width about 65 ± 5%.
3. A considerable reduction in calcium hydroxide content "CH" is documented in concrete mixture containing crystalline additive materials; this may be due to the presence of highly fineness silica that can react with CH.
4. XRD analysis indicates that, the crystalline additives materials "CA" is mainly composed of cement, silica and carbonated materials.
5. TGA analysis reveals that, the CA materials mixed with pore solution shows decrease in CH amount compared to its relevant mixed with water.
6. The reduction percent on (S_i) for control specimens was significantly clear for concrete mixtures with 0.60 and 0.50 (w/c) ratios.
7. The higher the (w/c) ratios, the higher the efficiency of the using "CA" materials regarding the enhancement on the water capillary raise resistivity.
8. For impermeable concrete ;(i.e. Low w/c ratio); there is no need of using CA materials, where, no significance difference in (S_i) for concrete samples with and without CA materials.
9. Continuous water curing may result in a great enhancement of the concrete impermeability in case of using (CA) materials.

Declaration of Competing Interest

The authors declare that they have no known competing financial interests or personal relationships that could have appeared to influence the work reported in this paper.

References

[1] R. Kumar, B. Bhattacharjee, Porosity, pore size distribution and in situ strength of concrete, Cem. Concr. Res. 33 (1) (2003) 155–164.
[2] ACI Committee 212, A.R.-R.o.C.A.f.C. and American Concrete Institute.
[3] J. Pazderka, E. Hájková, Crystalline admixtures and their effect on selected properties of concrete, Acta Polytech. 56 (4) (2016) 306–311.
[4] Y. Yang et al., Autogenous healing of engineered cementitious composites under wet–dry cycles, Cem. Concr. Res. 39 (5) (2009) 382–390.
[5] L. Ferrara, V. Krelani, M. Carsana, A "fracture testing" based approach to assess crack healing of concrete with and without crystalline admixtures, Construct. Build. Mater. 68 (2014) 535–551.
[6] P. Azarsa, R. Gupta, A. Biparva, Assessment of self-healing and durability parameters of concretes incorporating crystalline admixtures and Portland Limestone Cement, Cem. Concr. Compos. (2019).
[7] K. Sisomphon, O. Copuroglu, E. Koenders, Self-healing of surface cracks in mortars with expansive additive and crystalline additive, Cem. Concr. Compos. 34 (4) (2012) 566–574.
[8] B. Park, Y.C. Choi, Prediction of self-healing potential of cementitious materials incorporating crystalline admixture by isothermal calorimetry, Int. J. Concr. Struct. Mater. 13 (1) (2019) 36.
[9] L. Ferrara, Self-healing cement-based materials: an asset for sustainable construction industry. In: IOP Conference Series: Materials Science and Engineering, 2018. IOP Publishing.
[10] Z. Jiang et al., Self-healing of cracks in concrete with various crystalline mineral additives in underground environment, J. Wuhan Univers. Technol.-Mater. Sci. Ed. 29 (5) (2014) 938–944.
[11] M. Wu, B. Johannesson, M. Geiker, A review: self-healing in cementitious materials and engineered cementitious composite as a self-healing material, Construct. Build. Mater. 28 (1) (2012) 571–583.
[12] N. Žižková, Š. Keprdová, R. Drochytka, The use of secondary crystallization in cement-based composites, Int. J. Civil Environ. Eng. 10 (12) (2016) 1570–1573.
[13] ASTM C1585-13, Standard Test Method for Measurement of Rate of Absorption of Water by Hydraulic-Cement Concretes, in 2013: ASTM International, West Conshohocken, PA, 2013, www.astm.org. pp. 6.
[14] F. Pacheco-Torgal et al., Eco-efficient Repair and Rehabilitation of Concrete Infrastructures, Woodhead Publishing, 2017.
[15] W. Kurdowski, Cement Hydration, in Cement and Concrete Chemistry, Springer Netherlands, Dordrecht, 2014, pp. 205–277.
[16] Z. Li, in: Structure of Concrete, in Advanced Concrete Technology, John Wiley & Sons, Inc, 2011, pp. 140–163.
[17] A. Nonat, The structure and stoichiometry of C-S-H, Cement and Concrete Research 34 (9) (2004) 1521–1528.
[18] L. Zhang et al., Novel understanding of calcium silicate hydrate from dilute hydration, Cem. Concr. Res. 99 (2017) 95–105.
[19] P. Hou et al., Characteristics of surface-treatment of nano-SiO2 on the transport properties of hardened cement pastes with different water-to-cement ratios, Cem. Concr. Res. 55 (2015) 26–33.
[20] J.W. Bullard et al., Mechanisms of cement hydration, Cem. Concr. Res. 41 (12) (2011) 1208–1223.
[21] D. Hou, H. Ma, Z. Li, Morphology of calcium silicate hydrate (C-S-H) gel: a molecular dynamic study, Adv. Cem. Res. 27 (3) (2015) 135–146.
[22] D. Kong et al., Whether do nano-particles act as nucleation sites for C-S-H gel growth during cement hydration?, Cem. Concr. Compos. 87 (2018) 98–109.
[23] M. Stefanidou, I. Papayianni, Influence of nano-SiO2 on the Portland cement pastes, Compos. Part B Eng. 43 (6) (2012) 2706–2710.
[24] Z. Jiang, W. Li, Z. Yuan, Influence of mineral additives and environmental conditions on the self-healing capabilities of cementitious materials, Cem. Concr. Compos. 57 (2015) 116–127.
[25] U. Sharma et al., Effect of particle size of nanosilica on microstructure of C-S-H and its impact on mechanical strength, Cem. Concr. Compos. 97 (2019) 312–321.